International Conference on Space Optics—ICSO 2010

Rhodes Island, Greece

4–8 October 2010

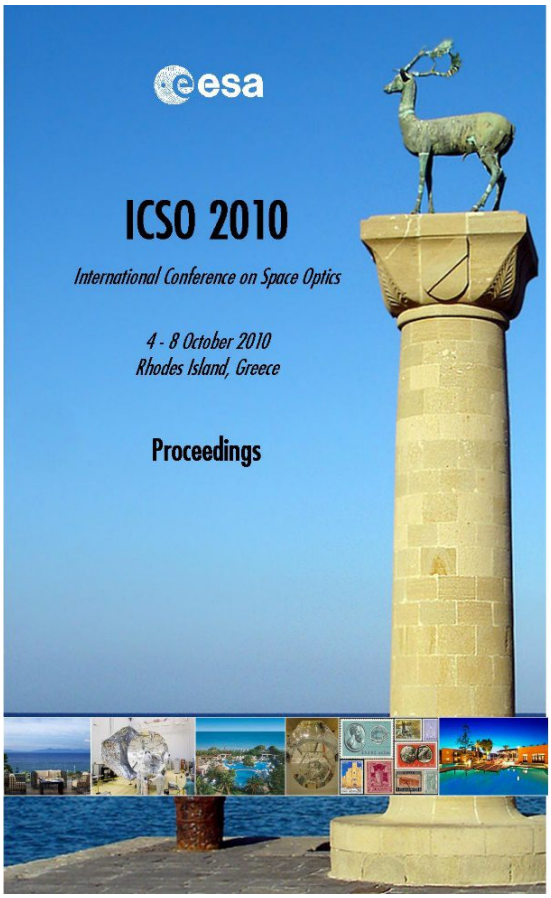

Edited by Errico Armandillo, Bruno Cugny, and Nikos Karafolas

Status of backthinned AlGaN based focal plane arrays for deep-UV imaging

J.-L. Reverchon, G. Lehoucq, J.-P. Truffer, E. Costard, et al.

International Conference on Space Optics — ICSO 2010, edited by Errico Armandillo, Bruno Cugny, Nikos Karafolas, Proc. of SPIE Vol. 10565, 1056509 · © 2010 ESA and CNES
CCC code: 0277-786X/17/$18 · doi: 10.1117/12.2309156

STATUS OF BACKTHINNED ALGAN BASED FOCAL PLANE ARRAYS FOR DEEP-UV IMAGING

J.L. Reverchon[1], G. Lehoucq[1], J.P. Truffer[1], E. Costard[1], E. Frayssinet[2], F. Semond[2], J.Y. Duboz[2], A. Giuliani[3], M. Réfrégiers[3], M. Idir[3].
[1]Thales Research & Technology & 3-5lab, France, [2]CNRS-CRHEA, France, [3]Synchrotron Soleil, France.

I. INTRODUCTION

The achievement of deep ultraviolet (UV) focal plane arrays (FPA) is required for both solar physics [1] and micro electronics industry. The success of solar mission (SOHO, STEREO [2], SDO [3]…), has shown the accuracy of imaging at wavelengths from 10 nm to 140 nm to reveal effects occurring in the sun corona. Deep UV steppers at 13 nm are another demanding imaging technology for the microelectronic industry in terms of uniformity and stability. A third application concerns beam shaping of Synchrotron lines [4]. Consequently, such wavelengths are of prime importance whereas the vacuum UV wavelengths are very difficult to detect due to the dramatic interaction of light with materials.

The fast development of nitrides has given the opportunity to investigate AlGaN as a material for UV detection. Camera based on AlGaN present an intrinsic spectral selectivity and an extremely low dark current at room temperature. We have previously presented several FPA dedicated to deep UV based on 320 x 256 pixels of Schottky photodiodes with a pitch of 30 µm [4, 5]. AlGaN is grown on a silicon substrate instead of sapphire substrate only transparent down to 200 nm.

After a flip-chip hybridization, silicon substrate and AlGaN basal layer was removed by dry etching. Then, the spectral responsivity of the FPA presented a quantum efficiency (QE) from 5% to 20% from 50 nm to 290 nm when removing the highly doped contact layer via a selective wet etching. This FPA suffered from a low uniformity incompatible with imaging, and a long time response due to variations of conductivity in the honeycomb. We also observed a low rejection of visible. It is probably due to the same honeycomb conductivity enhancement for wavelength shorter than 360 nm, i.e., the band gap of GaN.

We will show hereafter an improved uniformity due to the use of a precisely ICP (Inductively Coupled Plasma) controlled process. The final membrane thickness is limited to the desertion layer. Neither access resistance limitation nor long response time are observed. QE varies from 5% at 50 nm to 15% at 6 nm (85% more when taking into account the filling factor). Consequently, we can propose prototypes concerning not only "solar blind" camera optimized for narrow band in the near UV range (between 280 nm and 260 nm), but also devices with spectral range extended in the deep UV (290 nm to 10 nm). Both detectors are available for an optical budget evaluation.

II. FIRST PROTOTYPES

A. Process for deep UV extension

Processing has been extensively presented in reference [4]. It consists in a hybrid FPA whose range of detection is extended from near UV to deep UV. It is based on 320 x 256 pixels of Schottky photodiodes with a pitch of 30 µm. AlGaN is grown on a silicon substrate instead of sapphire substrate only transparent down to 200 nm. The architecture of the detector is based on an undoped active layer with an aluminum content of 35% and a n doped window layer with an aluminum content of 55%. A n doped gradual alloy prevents any conduction and valence band discontinuity between the window and active layers. The presence of a thick and doped window layer limits the spectral bandwidth to 20-25 nm. Basal AlN / GaN multilayer are incorporated for material improvement. But its final removal doesn't impact the final optoelectronic properties as long as it isn't exposed to light and exposed to access resistance variations.

The fabrication of an AlGaN 2D array on silicon is similar to that of an AlGaN 2D array on sapphire. It consists in mesa etching, ohmic and Schottky contact definition, passivation with dielectric, contact pads deposition, dicing and hybridization to readout circuit. As usual with nitride components, a strong mechanical stress arises during the epitaxy and induces a strong bowing. The bowing of AlGaN layers grown on silicon is larger than 45 µm for a 2 inch wafer. It requires a particular attention during processing.

After a flip-chip hybridization, silicon substrate is thinned and finally removed by ICP etching. The use of a honeycomb structure straightens the membrane after hybridization in order to allow the membrane integrity all along processing and stress tests. The results show that the dry etching process doesn't affect the readout circuit

properties. The dark current is negligible and we measured noise due to the large capacitance of the photodiode. We also benefit from 3-5 ICP to continue etching close to the gradual and active layers. A key parameter is the temperature kept under 80°C requested for indium bump compatibility and control of crack expansion across layers. Another advantage is its anisotropy and the capability to create a honeycomb structure in order to limit the expansion of cracks.

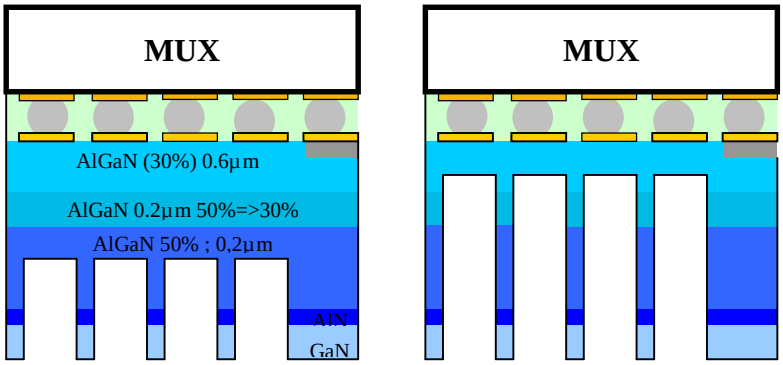

Fig.1. Sketch of the FPA adapted to deep UV before(left) and after wet etching (right).

B. First optoelectronic results

We measured a QE of 35% at 300 nm for which the window layer is transparent and absorption takes place in the active layer very close to the Schottky contact. When the wavelength is lower, i.e. 260-300 nm, the absorption takes place in the window layer and closer to the backside surface. The QE decreased down to several percents. It means that carriers were immediately recombined in the highly doped layer.

As it was not possible to begin a new dry etching by ICP due to the high risk of failure, we consequently tested a local wet photochemical etching. Silicon honeycomb was preliminarily etched. Then the highly aluminum and silicon doped AlGaN layer (200 nm window and gradient alloy layers) were selectively eliminated [5].

C. Optoelectronic properties after chemical etching

The effect of wet etching on the enhancement of QE is obvious on figure 2, left. But several drawbacks take place. First, the contribution corresponding to GaN band-gap, i.e. 360 nm, is due to a lower access resistance when carriers are generated in the GaN based honey-comb. Second, a long response time follows the fast responsivity as shown in figure n°2 (right). Such effects may be due to the versatile access resistance in the honeycomb but also to a high doping level in the active layer prompt to deep level activation. When acquiring signal with integration time shorter than 10 ms, this slow activation is negligible and the only measured signal is the fast component.

A readout noise around 340 electrons rms was measured [5]. This value is high compared to the 150 electrons rms noise measured with AlGaN on sapphire camera. Compared to the readout circuit noise measured at 45 electrons with unconnected pixels, the excess noise is suspected to be due to the high capacitance of photodiodes. This high value is achieved by the low desertion layer due to a high doping level. Indeed, n doping is achieved by silane. This gas is present in the growth chamber after the intentionally doped layers growth (window and gradual layers) and induces a large residual doping.

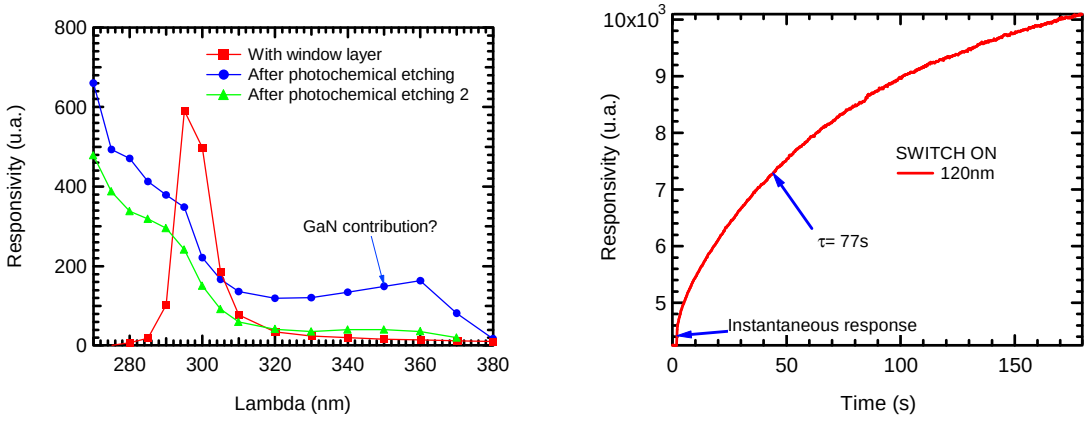

Fig.2. Effect of photo-chemical etching on near UV spectra (left) and response time (right)

D. Responsivity in the deep UV range

The QE is estimated from the fast component of the photocurrent. The spectral responsivity of this focal plane array presented a QE from 10% to 20% from 130 nm to 290 nm after the removal of the highly doped contact layer. We observe in figure n°3 a QE around 1% from 310 nm to 360 nm due to the activation of the GaN layer in the honeycomb. These values consist in an optimistic results but need to be clarified. But some strong improvement in terms of rejection of visible and elimination of long response time are required.

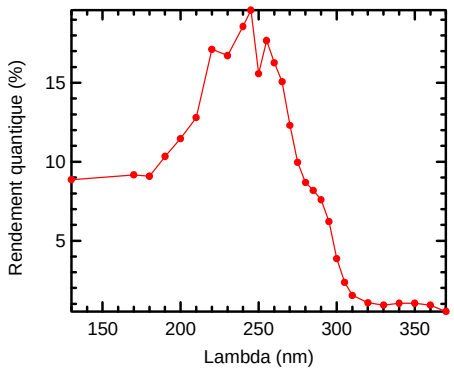

Fig. 3. Spectral responsivity from 130 to 360 nm.

III. FPA FABRICATION WITH IMPROVED PROCESS

A Fabrication

The epitaxial material is similar to the wafer involved in previous attempts. It consists in a AlN / GaN / AlN / $Al_{.6}Ga_{.4}N$ / $Al_{.4}Ga_{.6}N$ multilayers. The aluminum content in both active and window layers is increase by 5% in order to approach solar blind devices properties in terms of dark current and noise figure. We paid attention on the solid state doping instead of silane based doping suspected to induce high capacitance and readout noise.

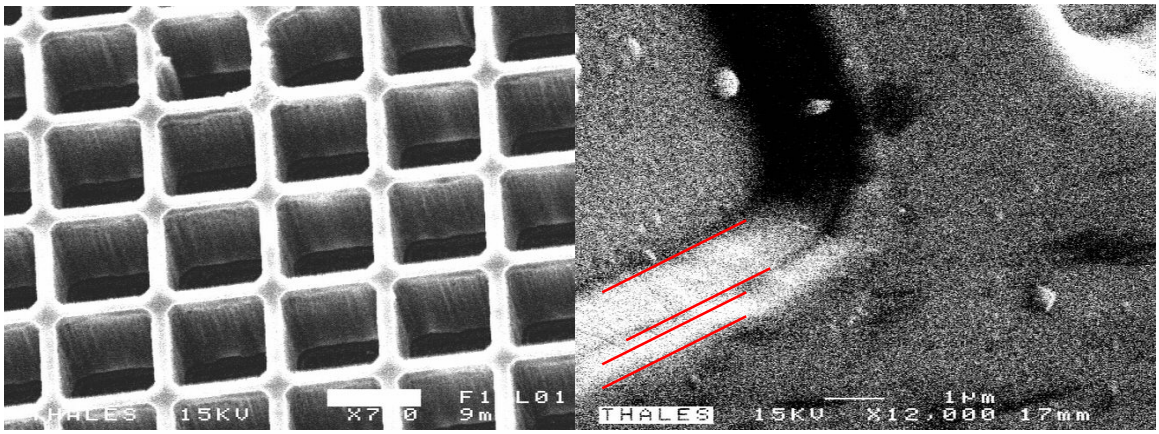

Fig. 4. Silicon honeycomb after ICP etching. (left). AlGaN / AlN / GaN honeycomb after silicon removal for SEM acquisition

Several honeycomb thicknesses from 7 to 8 µm are tested in order to improve filling factor and robustness. A honeycomb structure is shown in figure 4. The dark layer reveals the AlN layer just below the window layer. A set of 4 FPA was fabricated in order to determine the best stabilized conditions for the next set of 8 FPA. After silicon etching the devices with the narrowest honeycomb and thinnest thickness (i.e. those extracted from the edge of the wafer: R08C07-D3 and R08C06-D2) revealed a high density of cracks. Few cracks appear during honey-comb etching in AlGaN. Such a density of crack is crippling for future use in harsh environment. Consequently, the AlGaN etching was subdivided in steps of 1 minute in order to avoid a dramatic increase of temperature for indium bumps. Then, the next set of 8 representative FPA will be defined with larger honeycomb safer for membrane robustness: 10 µm corresponding to a filling factor of 45%.

B. Electrical properties

Some of the electrical properties are summarized in table 1. The cracks are contributing to the average dark current and short cuts showing the necessity to avoid it. Unconnected pixels will have to be solved by planarity concern. Future micro-section analyze will define whether indium bump suffer from two ICP etching in silicon and (Ga,Al)N.

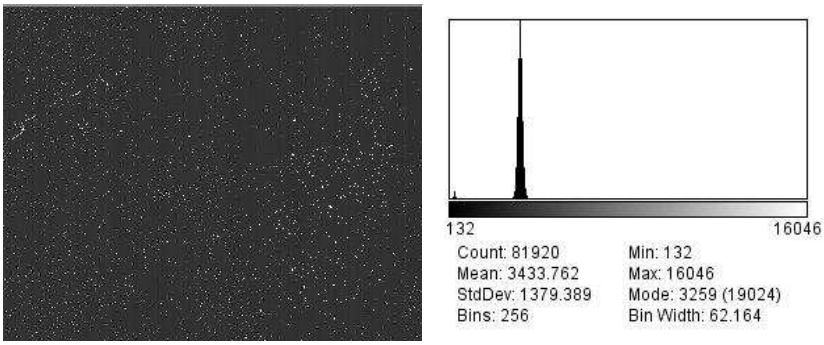

Fig.5. Cartography and histogram of backthinned AlGaN (R08C07-D3, gain 16µV/e-, integration time: 10 ms)

Number of FPA	R08C07-D3	R08C05-C3	R08C04-B3	R08C06-D2
Membrane's thickness	450 nm	450 nm	400 nm	350 nm
Cracks	1	1	20	>40
Short cut pixels	0,6 %	0,4 %	0,4%	0,9 %
Non connected pixels	2,1 %	1,95 %	1,8 %	1,6 %
Dark current	20 000 e-/s	50 000 e-/s	26 000 e-/s	90 000 e-/s
Noise 10 ms	175 e- rms	179 e- rms	155 e- rms	190 e- rms

Tab.1. Electrical features measured on 4 devices dedicated to etching optimization

C. Spectral responsivity

- *Near UV properties*

The near UV spectral properties are presented in figure 6. We observe a rejection of visible wavelengths larger than 4 orders of magnitude limited by internal fluctuations in Schottky contact [6], a sharp cut-off at 300 nm limited by alloy fluctuations in (Ga,Al)N [7]. Future architectures dedicated to larger rejection of visible are under design. On the contrary, the responsivity at wavelength lower than band gap (300 nm with 40% of aluminium content) is particularly flat except below 250 nm for which the calibration with Xenon lamp in the air is difficult. As a first conclusion, ***the highly doped gradient layer has to be completely removed***.

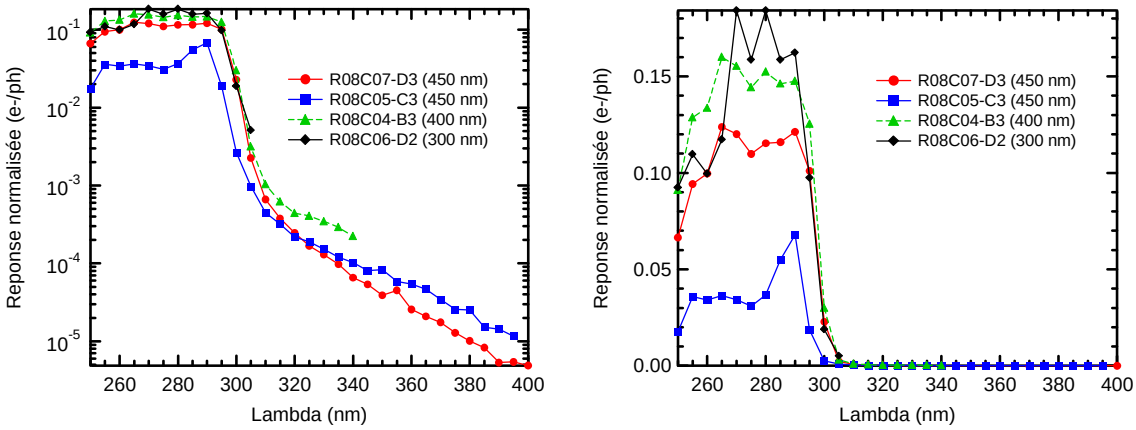

Fig.6. Spectral responsivity with logarithmic (left) and linear scale (right)

- *Deep UV properties*

Photoresponse spectra from 50 eV (25 nm) to 220 eV (6 nm) have been achieved owing to the synchrotron line Metrology X-UV from Soleil. We observe in the next figure a QE larger than 100% (1 e-/ph) with energies larger than 120 nm. This is due to multi-excitation when photon energy is larger than 3 times the band-gap energy. Most of the differences of QE are explained by the membrane's thickness. 450 nm is too thick to avoid recombination in the gradient layer (R08C07-D3 is an exception). The thinnest membrane of 300 nm gives the best results, but the numerous cracks induce access resistance's limitations and saturation effects. We observe a slightly better QE with R03C04 (wet etched FPA from chapter II) from 12 nm to 21 nm. This effect has to be considered with caution. An unexplained spectral feature took place. Some signal is added to the diffracted order in the incoming signal. Consequently, ***400 nm is the best tradeoff between membrane's robustness and QE in deep UV***.

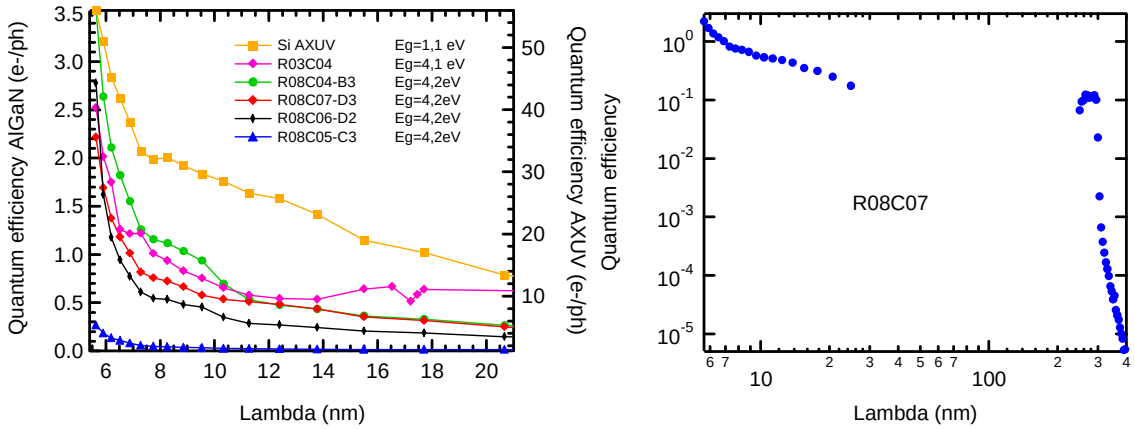

Fig.7. Quantum efficiency and efficacy of collection from 50 eV (25 nm) to 220 eV (6 nm)

Then, we define the collection efficiency as the ratio QE/3hν to avoid multi-excitation effects when photon energy exceed the band gap energy. We still observe figure 8 an increase of collection efficiency correlated to the deeper penetration of photon in the AlGaN membrane as shown in the cartography of figure 8 (right).

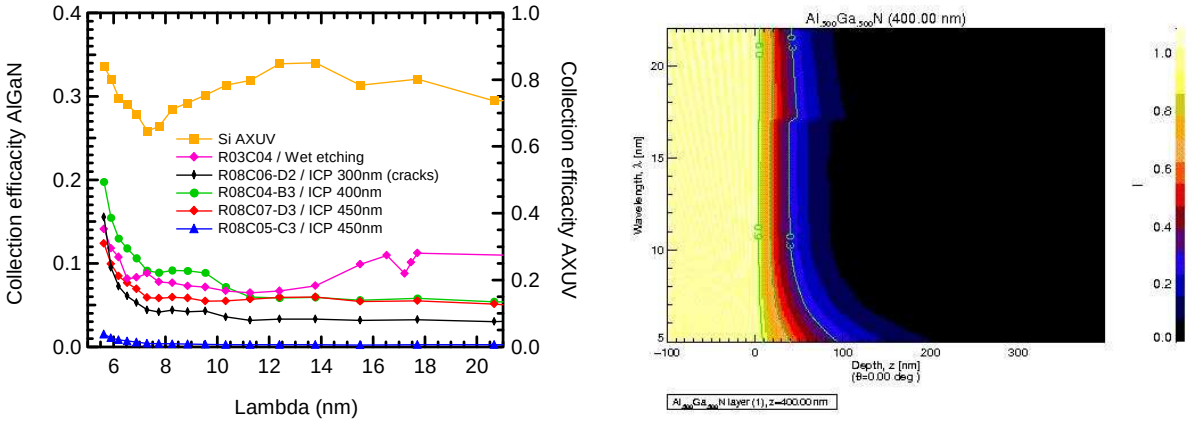

Fig.8 Left: Collection efficiency; and Right: Cartography of electric field intensity I in AlGaN membrane depth (abscises) versus wavelength (vertical)

- *Response time*

Another interesting improvement due to the dry etching is the fast response time observed for all 4 samples and presented figure 9 for several energies with FPA number R08C07-D3. We don't observe any overshot but a tiny increase of responsivity. When switch off, the signal comes to near zero immediately. A component of few seconds of less than few percents of the total signal is observed for all samples.

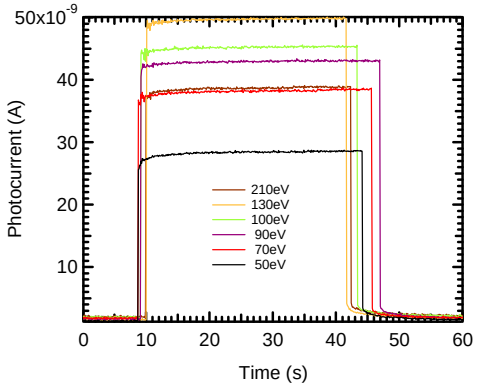

Fig.9. Response time of 2D array to synchrotron signal with photon energy from 50 to 210 eV

- *Responsivity after long irradiation:*

In order to check the behaviour of our device in harsh environments, we have measured the responsivity of our device under a large flux from the metrology line just filtered with a Lyman α filter. Quantitative measurements are suspicious due to parasitic features observed in images and spectra. The estimation of 1% is

too low compared to the results observed with the first prototype chemically etched. It will be precisely measured by a continuous spectra from visible to 50 nm in the DISCO line in early September. Nevertheless, we observe a slow decrease of signal after a fluence about 10^{16} photons/cm². A comparison of behaviour with the state of art silicon photodiodes from AXUV [8] is interesting. Indeed, silicon based photodiodes with a SiO_2 passivation show similar behaviour with equivalent fluence. Some preliminary explanation could be a dead layer, a thin oxide or even localized defects and traps in bulk AlGaN.

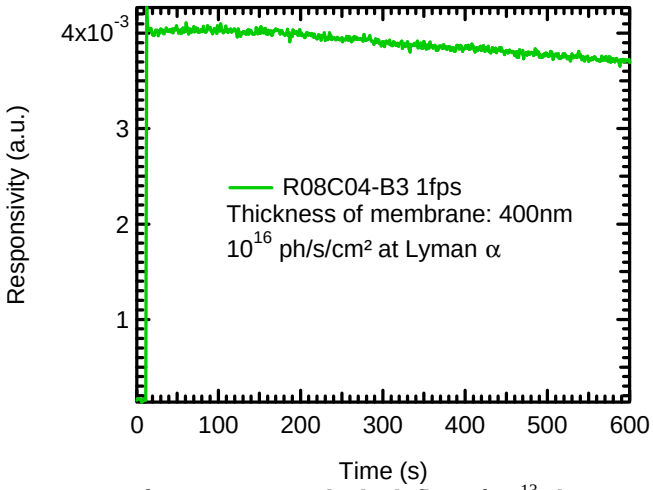

Fig.10. Decrease of responsivity under high flux of 10^{13} ph/s/cm² at 120 nm

IV. CONCLUSION

Capability to achieve a robust back thinned AlGaN FPA with honeycomb, uniformity and a quantum efficiency in the 5% to 20% range has been shown. A membrane's thickness of 400 nm without any doped layer is a convenient tradeoff in terms of robustness and deep UV QE. Such FPA doesn't suffer from smearing and allow high frame rate imaging. QE from 250 nm to 60 nm, particularly for Lyman α, will soon be precisely measured. In a second phase, a set of 8 FPA will be fabricated in order to check the reliability of the process. We will also lead some climatic tests and thermal cycling in order to follow dark current, optical responsivity and robustness of the AlGaN membrane. The compatibility of honeycomb features with shorter pitch is not an issue as we expect the filling factor to be the only parameter conditioning the membrane's robustness. We stress that such an honeycomb feature allows new architecture of pixels insensitive to internal photoemission in contacts and useful for the shielding in harsh environment. Due to this honeycomb, filling factor is reduced to 55% and limits the quantum efficiency. Nevertheless an enhancement by micro lenses is possible as long as transparent materials are available.

V. ACKNOWLEDGEMENTS

Thanks are due to CNES for its project number R-S08SU-0004-029 for the development of deep UV arrays. We acknowledge SOLEIL for provision of synchrotron radiation facilities and particularly the beam lines Metrology and DISCO.

VI. REFERENCES

[1] J.F. Hochedez et al. ,"New UV detectors for solar observations", proced. SPIE (2002)
[2] http://smsc.cnes.fr/STEREO/index.htm
[3] http://sdo.gsfc.nasa.gov/
[4] J.L Reverchon, S. Bansropun, J.P., Truffer, E. Costard, E. Frayssinet, F. Semond, J.Y. Duboz, M. Idir, A. Giuliani, ," Performances of AlGaN based focal plane arrays from 10 nm to 200 nm", *Proc. SPIE*, 7691-07 (2010).
[5] J.L Reverchon, S. Bansropun, J.A. Robo, J.P. Truffer, E. Costard, E. Frayssinet, J. Brault, F. Semond, J.Y. Duboz, M. Idir, "First demonstration and performance of AlGaN based focal plane arrays for deep-UV imaging", Proc. SPIE 7474-54 (2009).
[6] J-Y. Duboz, N. Grandjean, F. Omnès, M. Mosca, J-L. Reverchon, " Internal Photoemission in AlGaN Solar blind detectors" Appl. Phys. Lett. 86, 063511 (2005).
[7] J.L. Reverchon, G. Mazzeo, A. Dussaigne and J.Y. Duboz, *Proc. SPIE* n°6398-25 (2005)
[8] http://www.ird-inc.com/brochure/IRD2010.pdf